

GPS Carrier-Phase Time Transfer Boundary Discontinuity Investigation

Jian Yao and Judah Levine

Time and Frequency Division and JILA, National Institute of Standards and Technology and University of Colorado, Boulder, Colorado 80305, USA

jian.yao@colorado.edu

Abstract—We report on a study of the carrier-phase time transfer boundary discontinuity by the use of the precise point positioning (PPP) technique. Carrier-phase time transfer is first compared with two-way satellite time and frequency transfer (TWSTFT) between the same stations. It matches TWSTFT quite well and provides better short-term stability. Later, we extract 1-day data-arc boundary discontinuity jump values for 151 days. The distribution of jump values is almost Gaussian. Different GPS receivers have different mean jump values (-200 ps to +200 ps) and different standard deviations (100 ps to 300 ps). Among the receivers at NIST (USA), USNO (USA), and PTB (Germany), USNO has the smallest absolute mean jump value (14.2 ps) and the smallest deviation (105.1 ps). In addition, with the increase of data-arc from 1-day to 4-days, both mean value and deviation increase. For receivers at the same station, the correlation varies. At PTB, the correlation between the jumps for receivers PTBB and PTBG is only -0.064. At NICT (Japan), the correlation between receivers SEPA and SEPB is 0.47, while that between receivers SEPB and SEPT is 0.10. The above variation in the correlation between receivers at the same location suggests that the boundary discontinuity does not mainly come from satellite-path-related noise. Further investigation reveals that multipath also contributes little to boundary discontinuity. Comparison between PPP and network method shows that the algorithm of fixing phase ambiguity plays an important role in boundary discontinuity.

Key words: *GPS, carrier-phase, time transfer, boundary discontinuity, precise point positioning*

I. INTRODUCTION

Global Positioning System (GPS) carrier-phase (CP) measurements are currently a widely accepted method for high precision time transfer [1, 2]. The method provides lower short-term noise than other time transfer methods, such as Two Way Satellite Time and Frequency Transfer (TWSTFT) and Common View (CV) Time Transfer [3].

However, independent daily CP time transfer solutions frequently show boundary discontinuities of up to 1 ns due to the inconsistency of the phase ambiguity between two independent days. Although there are some post-processing methods [4, 5] that mitigate the discontinuity, the origin of the inconsistency of the phase ambiguity is still not very clear, which makes CP time transfer not very useful for comparing primary frequency standards and similar high-accuracy applications.

The GPS observation equations for code and CP measurements have the following form, respectively:

$$P_i^j = |\vec{x}^j - \vec{x}_i| + \Delta_{tropo} + \Delta_{ion} + c\Delta t_i - c\Delta t^j + \Delta MP_i^j + \epsilon, \quad (1)$$

$$L_i^j = |\vec{x}^j - \vec{x}_i| + \Delta_{tropo} - \Delta_{ion} + c\Delta t_i - c\Delta t^j + \Delta MP_i^j(\text{carrier}) + \epsilon(\text{carrier}) + \lambda N_i^j, \quad (2)$$

where Δt_i is the clock bias of station i , Δt^j is the clock bias of satellite j ; Δ_{tropo} and Δ_{ion} are the tropospheric delay and ionospheric delay, respectively; ΔMP_i^j is the multipath correction; ϵ is the noise

term; N_i^j is the phase ambiguity. The multipath and noise terms are different for code and CP measurements.

Code measurement is much noisier than CP measurement. It provides accurate but not very precise timing information, while CP measurement provides precise but less accurate timing information due to the uncertainty of the phase ambiguity N_i^j . Code measurements are used to help fix the phase ambiguity so that we have both accurate and precise time. The physical noise in code measurements can lead to an incorrect phase ambiguity, which can lead to a boundary discontinuity in the end. Another possible reason leading to an incorrect phase ambiguity is the algorithm that is used to fix ambiguity itself. In the precise point positioning (PPP) technique, the zero-difference ambiguity of a satellite-receiver pair or the single-difference ambiguity between two satellites is naturally not an integer value, due to the existence of the uncalibrated phase delays originating in the receiver and satellite [6]. This makes the resolution of ambiguities by PPP method lower than that by the network method, which uses double differences to determine the uncalibrated phase delays.

In this paper, we begin with details of GPS data processing. Then we compare CP time transfer with TWSTFT. In Section IV, we study the statistical behavior of the boundary discontinuity, especially the mean and the standard deviation (STD). In Section V, we explore the possible physical noise in code measurement, e.g., multipath, the satellite orbit, and the correlation of boundary discontinuity between two receivers at the same station. Furthermore, we compare the boundary discontinuity of the PPP method and the network method, which shows the importance of the algorithm that is used to fix the ambiguity.

II. GPS DATA PROCESSING

The NRCan PPP software [7] was run for several GPS receivers for more than 150 days. The default settings are as follows: “USER DYNAMICS” is set to “STATIC” because all receivers used in this paper are in static mode; we use International GNSS Service (IGS) rapid products (SP3 and CLK) and RINEX as the input files for NRCan PPP; the software solves for both the station position and the clock bias; the cutoff elevation is set to 10 degrees. We extract the backward data to get the clock bias because a calculation in this direction provides a better tropospheric delay estimate and the solutions converge better in backward mode.

We use two strategies to extract the boundary discontinuity [2]. The first strategy is called “Raw Method,” which computes the time difference between the average of 0:00 and 0:05 for each day and the average of 23:50 and 23:55 for the previous day, and then corrects for the slope during the 10 min time period. The second strategy is called “Overlapping Method,” which runs PPP first for two consecutive days independently, then runs PPP for the combined two days, and then extracts the difference between the first day and the combined two days $\Delta_{1 \rightarrow X}$ and the difference between the combined two days and the second day $\Delta_{X \rightarrow 2}$. Then $\Delta_{1 \rightarrow 2} = \Delta_{1 \rightarrow X} + \Delta_{X \rightarrow 2}$ gives the jump value between the two days (See Figure 1). These two discontinuity extraction strategies give us almost the same jump values. For the sake of consistency, we will keep using the Overlapping Method except that the Raw Method is used in Section V.3 because IGS does not provide the timing information for the combined two days.

III. COMPARISON BETWEEN CP AND TWSTFT

TWSTFT uses a modem to generate a pseudo-random code synchronized to the 1 Hz ticks of the local clock [3]. This code is used to modulate the “up-link” microwave carrier at about 14 GHz. After receiving this signal, the satellite re-transmits it on the “down-link” frequency at about 12 GHz. This signal is received at the remote end and converted back to 1 Hz ticks. The system is full-duplex and transmits signals in both directions simultaneously. Since contributions to the path delay (such as the tropospheric, the ionospheric, the satellite position and clock) are nearly the same for both directions, we can eliminate the delay and achieve a timing accuracy that is typically better than 1 ns.

It is good for us to compare the CP method with TWSTFT in order to make sure that we run the CP method properly. Figure 2 shows us the comparison of the two methods for 30 days. The y-axis is the time difference between NIST and PTB. The uncalibrated cable delay leads to a non-zero average of the time difference between the two stations for CP method. In order to compare CP and TWSTFT, the TWSTFT data have been shifted by -418.5 ns. We can see that CP matches TWSTFT very well. They have the same long-period variation, and CP provides much better short-term stability.

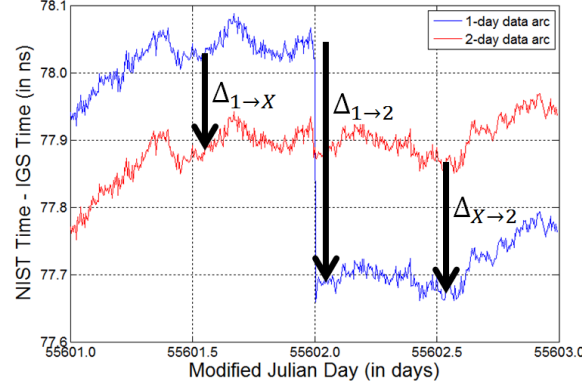


Figure 1. Algorithm of Overlapping Method. $\Delta_{1\rightarrow X}$ is the average time difference between the first day and the combined two days from 15:00 to 21:00. $\Delta_{X\rightarrow 2}$ is the average time difference between the second day and the combined two days from 3:00 to 9:00. $\Delta_{1\rightarrow 2} = \Delta_{1\rightarrow X} + \Delta_{X\rightarrow 2}$, where $\Delta_{1\rightarrow 2}$ is the jump value estimated by the Overlapping Method.

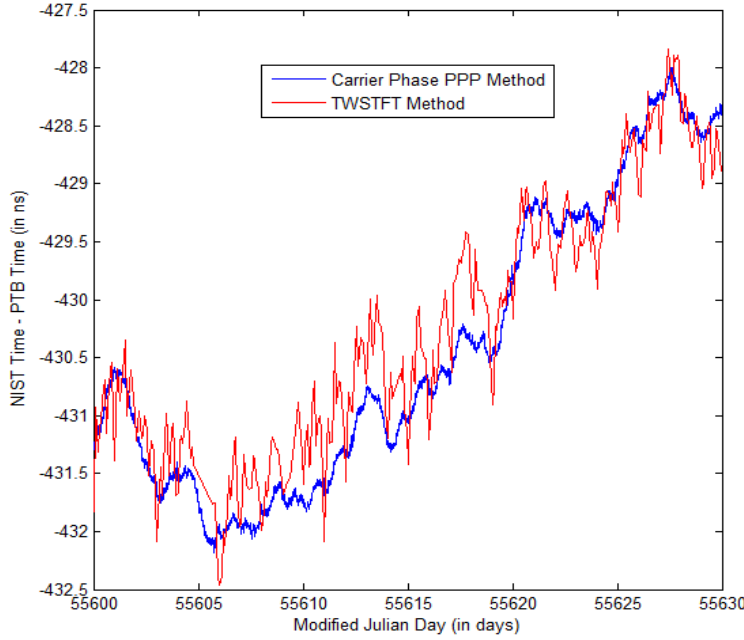


Figure 2. Comparison between carrier-phase time transfer and TWSTFT. TWSTFT has been shifted by -418.5 ns.

IV. STATISTICS OF BOUNDARY DISCONTINUITY

Figure 3 illustrates the UTC(NIST) clock bias with respect to the IGS time. Between Modified Julian Day (MJD) 55667 and MJD 55668, there is an adjustment in IGS time that leads to about a -7 ns jump. For all other days, we can see that there are many small jumps up to 1 ns. Before we explore the origin of these jumps, let us first study the statistics, e.g., the mean value and the STD of these jumps, and use statistics to describe these jumps. The statistics of jumps is also a touchstone for the improvement of the boundary

discontinuities. Figures 4 (a)-(c) are the histograms of the jump values for NIST, PTBB, and USN3 (in USNO), respectively. The distribution of the boundary discontinuities is almost Gaussian. The mean values are -146.7 ps, 45.4 ps and 21.4 ps, and the STDs are 236.7 ps, 138.5 ps and 106.7 ps. We can see that USN3 provides the smallest boundary discontinuity jump. The mean value of NIST is far from 0, which makes the popular concatenating algorithm difficult to implement [8].

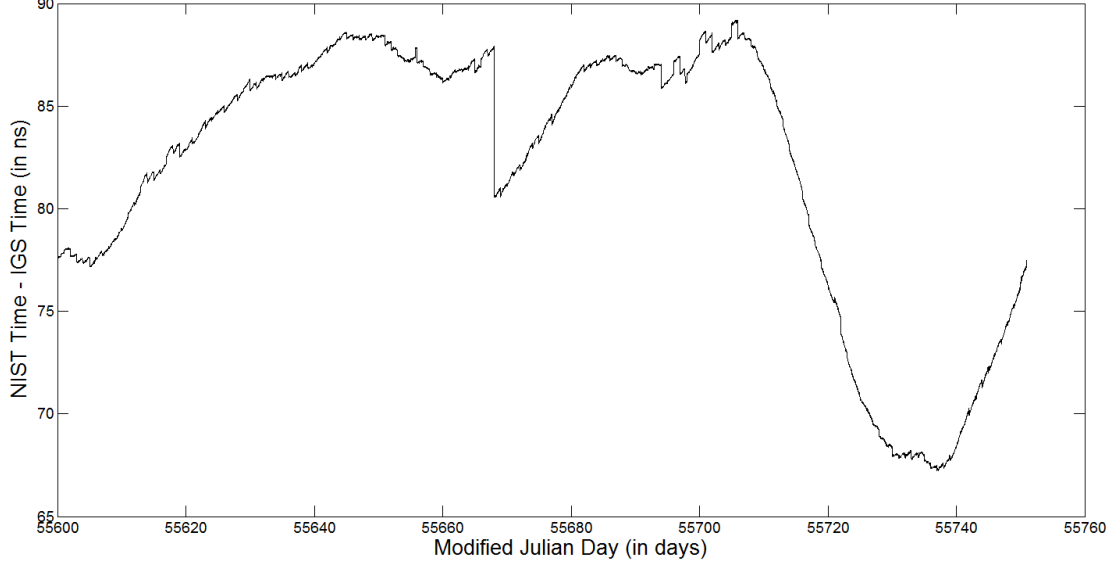


Figure 3. Time difference between UTC(NIST) and IGS Time over 151 days.

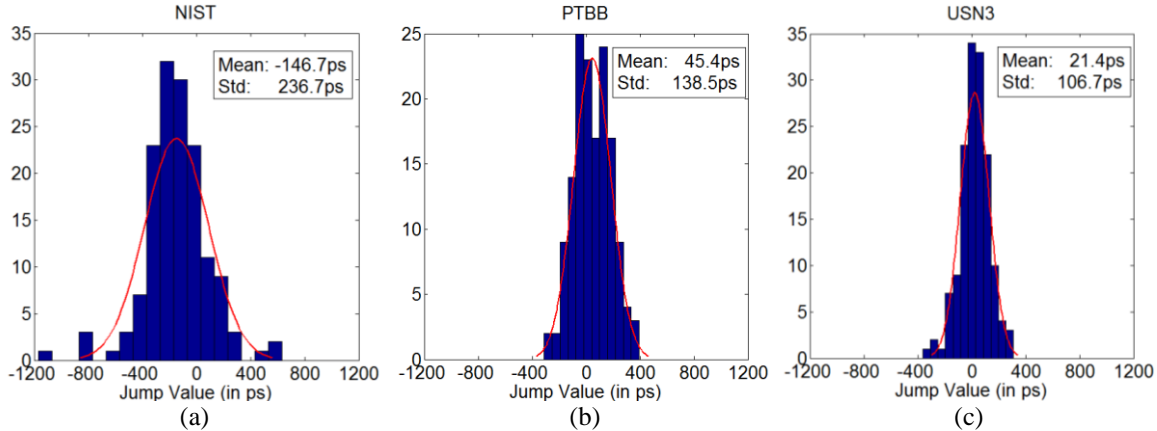


Figure 4. Histograms of jump values of NIST, PTBB, USN3 for MJD 55600-55750.

In Figure 4 are the statistics of the discontinuities for a data-arc of 1-day. The longer data-arc (e.g. 35 days) time transfer is accepted by many organizations, including BIPM [9]. Figures 5 (a)-(b) show the impact of longer data-arcs on the boundary discontinuity by running PPP for USN3 for MJD 55500-55900. Here, data-arcs range from 1-day to 4-days. Both the mean value and the STD of boundary discontinuity increase as the data-arc increases. That means that when a longer data-arc is used we should expect a greater boundary discontinuity. Theoretically, if the boundary discontinuity is an ideal independent white noise, we should have $\text{Mean} \propto \text{Data Arc}$ and $\text{STD}^2 \propto \text{Data Arc}$. The actual data in Fig. 5 (a)-(b) agree with this expectation.

V. ORIGIN OF BOUNDARY DISCONTINUITY

As stated in Section I, the boundary discontinuity may come from physical noise, or from the algorithm, or both. For physical noise, it can be separated into two categories. One is the satellite-path-related noise,

e.g., satellite orbit, satellite clock, tropospheric delay, and ionospheric delay. The other is the receiver-related noise, e.g., multipath, antenna, cable, and internal noise in the receiver circuits.

For receivers at the same station, the satellite-path-related noise should be almost the same. So the study of receivers at the same station can reveal how important the satellite-path-related noise is on the discontinuity, which is discussed in Part 1 of this section. Next, we explore the effect of multipath, an important receiver-related noise, in Part 2. Last, the PPP algorithm is compared with the network algorithm, in terms of boundary discontinuity. Other issues, such as the periodic behavior of discontinuity, are also discussed.

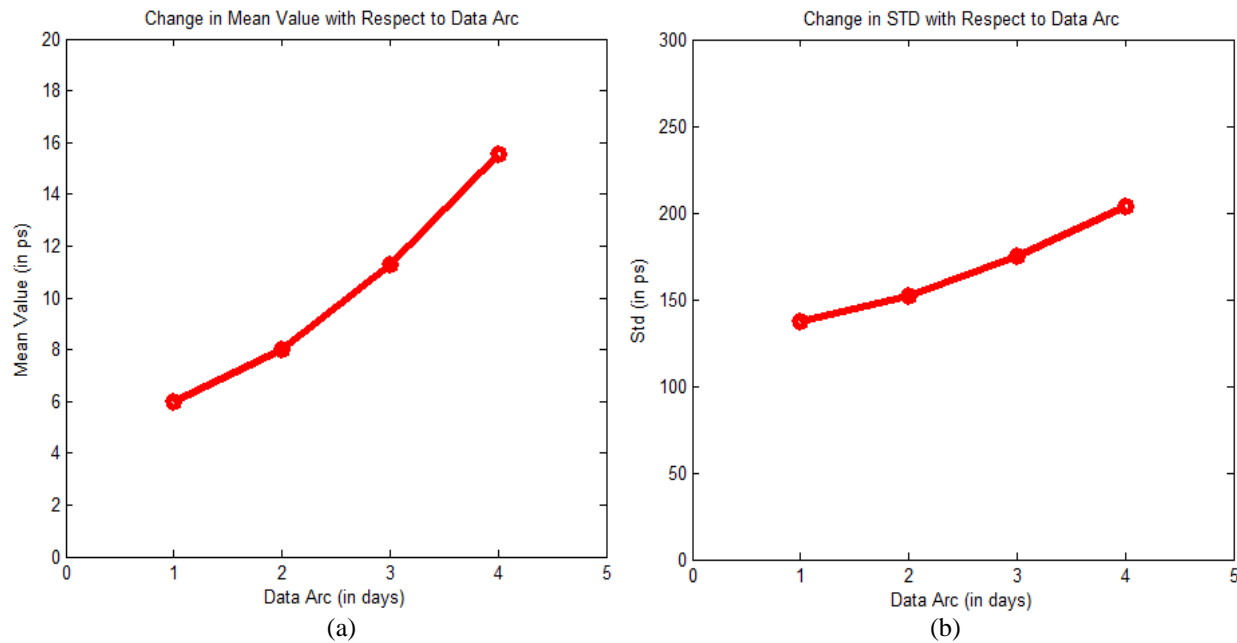


Figure 5. Statistics of boundary discontinuity of different data-arcs.

1. Boundary Discontinuity of Receivers at the Same Station

If the satellite-path-related noise plays an important role, the boundary discontinuity jump values of receivers at the same station should be highly correlated.

PTBB and PTBG are GPS receivers in PTB (See Figure 6(a)). Both of them are Ashtech Z-XII3T receivers. The distance between them is 6.51 m. Based on the statistics of jump values of MJD 55600-55750, the correlation coefficient between these two receivers is only -0.064, which is very close to 0. So the jump values of PTBB and PTBG are not correlated. This means that, compared with other noise, the satellite-path-related noise is so small that it has little impact on discontinuity. For SEPA, SEPB and SEPT in NICT (Japan), the correlation between SEPB and SEPT is only 0.102, which further confirms this conclusion. The totally different STD of SEPA and SEPT (see Figure 6(b)) also reveals that jump value has little relation with satellite-path-related noise. The high correlation between SEPA and SEPB could come from the receiver-related noise (e.g., multipath, cable noise, receiver circuits) or the algorithm of fixing phase ambiguity.

2. Multipath

Now that we have excluded the effect of the satellite-path-related noise on boundary discontinuity, let us explore the receiver-related noise. Multipath is of great importance. It varies from station to station.

Multipath in code measurement is usually at the level of a few meters. With the help of CP measurement, the bias due to multipath can still be at a several centimeters level, which can lead to 100 ps clock bias. Besides, although multipath repeats every 23 h 56 min, it is different every 24 h, which may lead to

different phase ambiguities between 2 days. So it is necessary for us to explore the impact of multipath on boundary discontinuity.

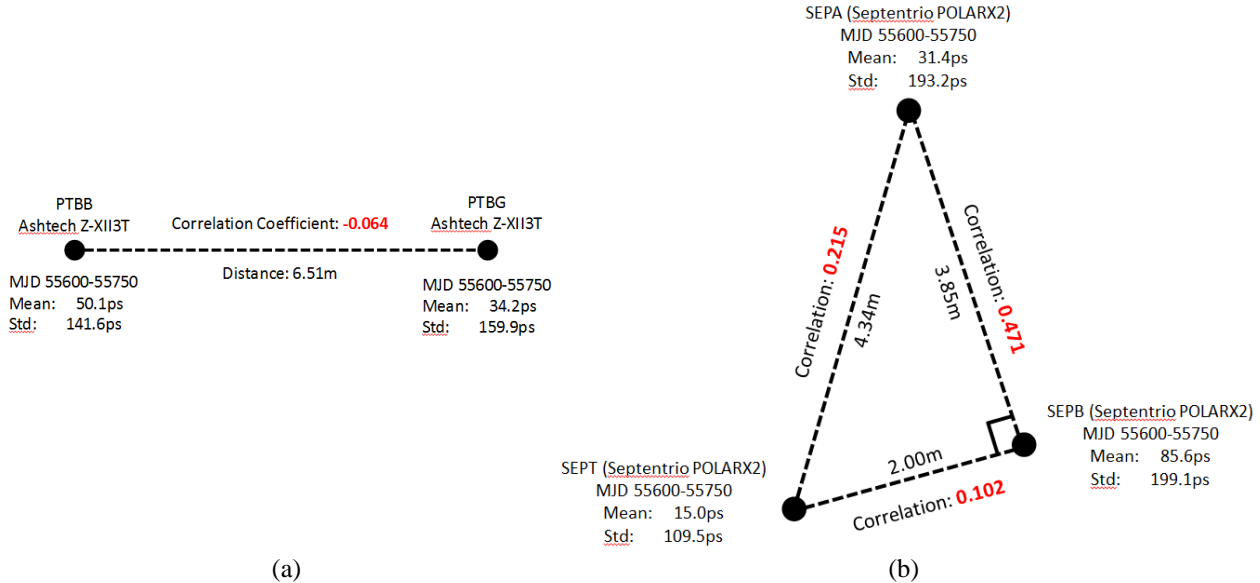


Figure 6. Correlation of boundary discontinuity of receivers at the same station. PTBB and PTBG are GPS receivers at PTB, Germany. SEPA, SEPB and SEPT are receivers at NICT, Japan.

Increasing the cutoff elevation has two impacts. On one side, it blocks some multipath from the low elevations which form the main part of the total multipath. So from this point of view, we should expect a decrease of boundary discontinuity, if multipath does affect boundary discontinuity. On the other hand, increasing the cutoff elevation reduces the visible satellite number, which leads to fewer observations, so it increases the uncertainty of the computed phase ambiguity. So from this point of view, we should expect an increase of discontinuity. However, this increase should be very small because low-elevation observations are given less weight than high-elevation observations. In sum, if the multipath affects our observation seriously, we should expect a big decrease of discontinuity as the cutoff elevation increases.

Figure 7 is the STD of boundary discontinuity of USN3, PTBB and SEPA at different cutoff elevations during MJD 55650-55850. We can see that the increase of cutoff elevation gives little improvement on boundary discontinuity. This illustrates that multipath, at least at USN3, PTBB and SEPA, is not an important factor on the magnitude of the boundary discontinuity.

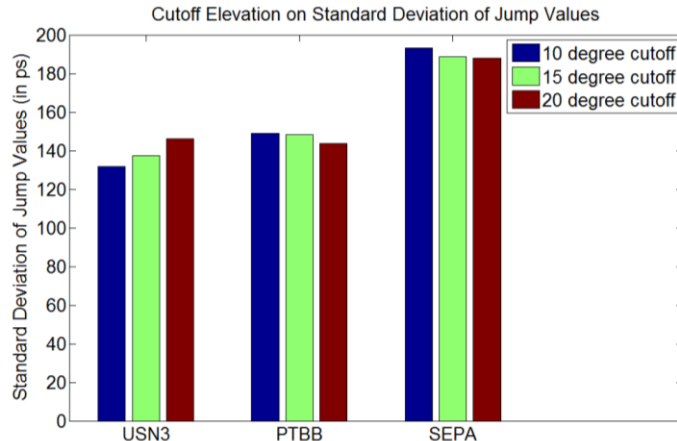


Figure 7. Effect of cutoff elevation on boundary discontinuity.

3. Algorithms of Fixing Ambiguity

In the PPP method, the receiver delay and the N satellites delays cannot be separated. In the N observations, we cannot resolve these $N+1$ unknown variables. So we need to set one delay to a specific value and solve for the other N variables. This makes it hard to resolve the phase ambiguity to an integer. In the network method, since we have other receivers (e.g., we have three receivers and three satellites in total), there are nine independent observations with six unknown cable delays for satellites and receivers. So we can solve these delays. This leads to a great improvement of fixing the ambiguity in eq. (2).

The IGS clock file has clock biases of many ground stations that are computed by the network method. So the IGS clock data should be considered as the network solution, which is compared with the PPP method, as shown in Figure 8. We can see that the mean jump value is closer to 0 in the network method than the PPP method. Furthermore, the STD is typically more than 20 ps smaller than with the PPP method. This means that the network method is better than the PPP method in terms of boundary discontinuity. Any improvement in the algorithm for fixing the ambiguity can give a smaller discontinuity, even though the noise in physical measurement is still the same.

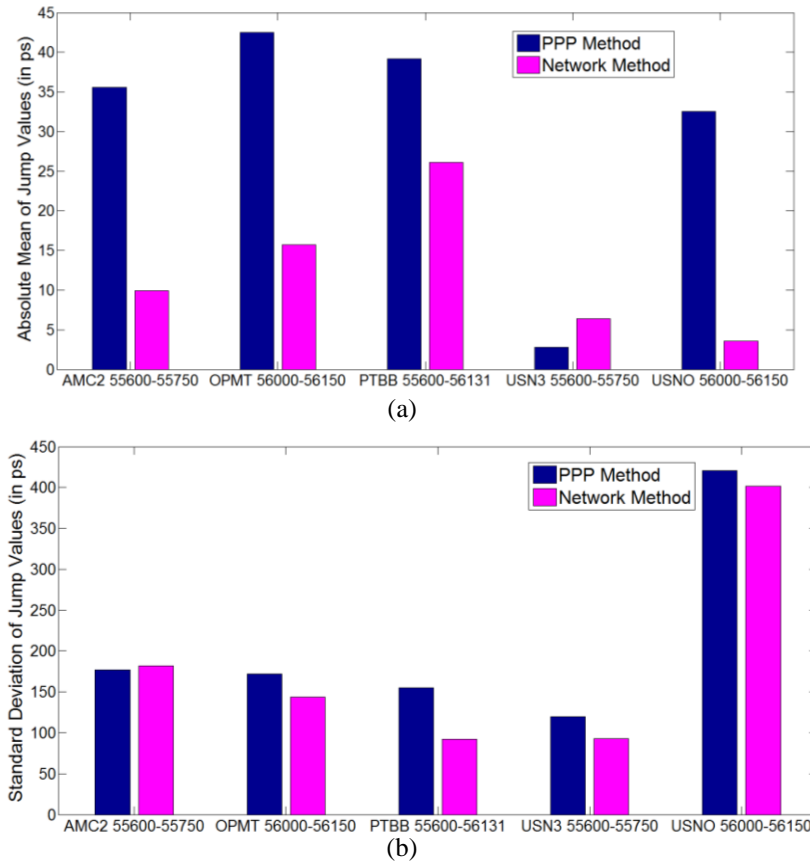


Figure 8. Effect of algorithms of fixing ambiguity on boundary discontinuity. Figure 8(a) shows the absolute mean of discontinuity of both the PPP method and the network method for five stations. Figure 8(b) shows the STD of discontinuity.

4. Other Issues

The boundary discontinuity behavior is not changed whether IGS final products or IGS rapid products are used. For PTBB from MJD 55600 to MJD 56017, the mean of jump values is 41.3 ps and the standard deviation is 147.2 ps when the IGS rapid products are used. Those values are 53.0 ps and 146.5 ps, respectively, when the IGS final products are used. This confirms our conclusion that the satellite-path-related noise is of little importance on the magnitude of the boundary discontinuity.

Figure 9 shows the long-term (more than 1000 days) boundary discontinuity. In February and August, there are some peaks in the jump values. In addition, as shown by the red curve, the period of boundary discontinuity is approximately one year. The peaks of jump values happen when the red curve reaches a local minimum (February) or maximum (August). The origin of the periodic behavior is still not clear. It may come from imperfect modeling of the tropospheric mapping function.

We have also run the PPP software in the position-fixed mode, which fixes the station at the initial input position and solves only for the clock bias. Running PPP in this mode leads to greater slope and greater boundary discontinuity in time transfer, when the initial input position is not at the right position (See Figure 10). The blue curve is the computed clock bias when the USN3 receiver is fixed at the right position. We can see that the boundary discontinuity is quite small in this case. However, when the receiver is fixed at a position with a -10 cm offset in X direction (black curve), the boundary discontinuity is more than 1 ns. The mean of the jump values is no longer near 0 ps.

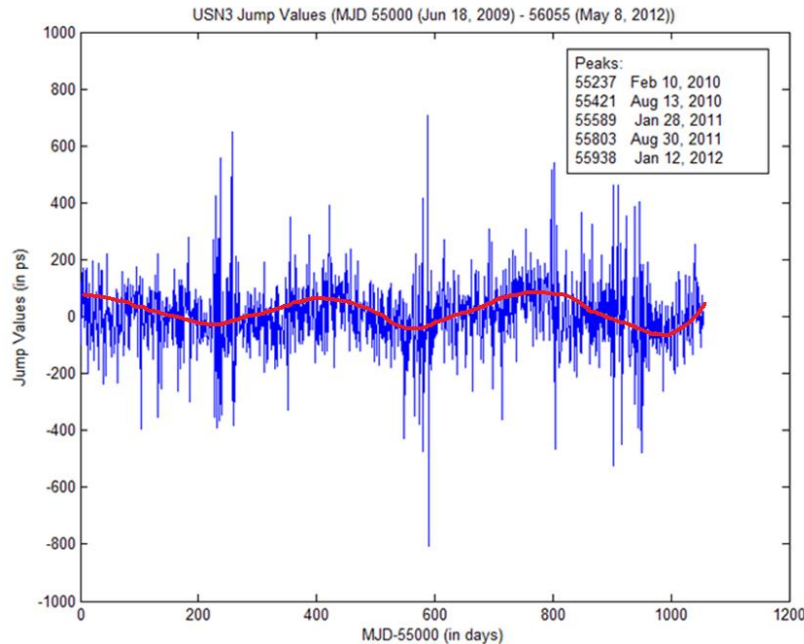


Figure 9. Long-term periodic behavior of boundary discontinuity. The start point of x-axis is MJD 55000.

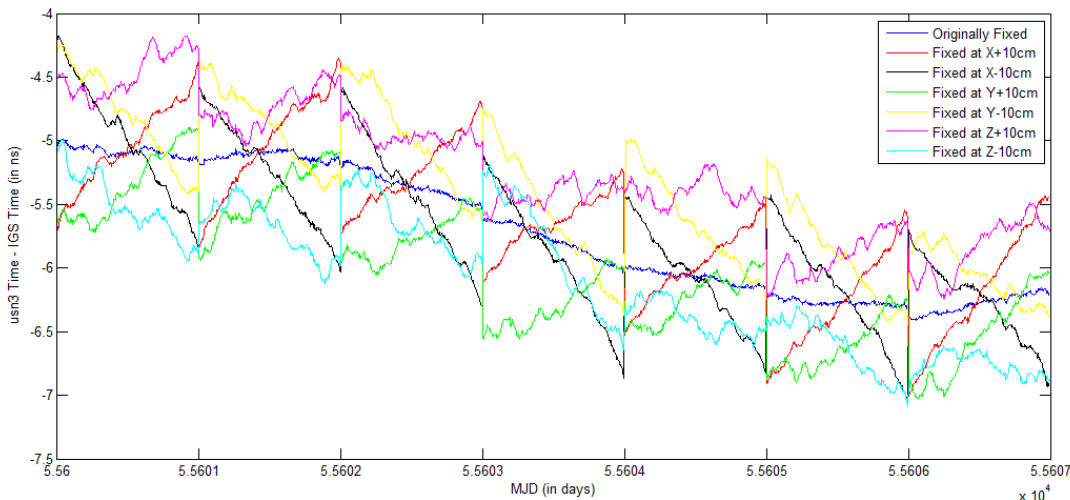


Figure 10. Effect of fixing receiver position on boundary discontinuity.

VI. CONCLUSIONS

Based on the above analysis, we know that the distribution of boundary discontinuity is almost Gaussian. Different GPS receivers have different mean jump values (ranging from -200 ps to 200 ps) and different standard deviations (100 ps to 300 ps). With the increase of data-arc from 1-day to 4-days, both mean value and standard deviation increase. So long-term data-arc carrier-phase time transfer should have a poorer discontinuity behavior.

For receivers in the same station, the correlation can be very small, which suggests that boundary discontinuity does not mainly come from the satellite-path-related noise. Further investigation reveals that multipath also contributes little to boundary discontinuity. Comparison between the PPP method and the network method shows that the algorithm of fixing phase ambiguity plays an important role in boundary discontinuity. Besides, the boundary discontinuity jump value has a period of approximately a year, which may come from imperfect modeling of the tropospheric mapping function.

VII. ACKNOWLEDGMENTS

The authors thank Francois Lahaye for sharing the NRCan PPP software. We also thank Thomas E. Parker for providing the TWSTFT data. Marc Weiss and Victor Zhang are thanked for some helpful discussions. IGS is gratefully acknowledged for providing GPS tracking data, station coordinates, and satellite ephemerides. Finally, we thank those people who maintain the GPS receivers in NIST, USNO, PTB, NICT, AMC2, and OPMT.

REFERENCES

- [1] K. M. Larson and J. Levine, "Carrier-phase time transfer," *IEEE Trans. Ultrason., Ferroelect., Freq. Contr.*, vol. 46, pp. 1001-1012, 1999.
- [2] C. Hackman, J. Levine, T. E. Parker, D. Piester, and J. Becker, "A straightforward frequency-estimation technique for GPS carrier-phase time transfer," *IEEE Trans. Ultrason., Ferroelect., Freq. Contr.*, vol. 53, pp. 1570-1583, 2006.
- [3] J. Levine, "A review of time and frequency transfer methods," *Metrologia*, 45, S162-S174, 2008.
- [4] R. Dach, T. Schildknecht, U. Hugentobler, L.-G. Bernier, and G. Dudle, "Continuous geodetic time transfer analysis method," *IEEE Trans. Ultrason., Ferroelect., Freq. Contr.*, vol. 53, no. 7, pp. 1250-1259, 2006.
- [5] K. Senior, E. Powers, and D. Matsakis, "Attenuating day-boundary discontinuities in GPS carrier-phase time transfer," *Proc. 31st PTTI Meeting*, pp. 481-490, 1999.
- [6] M. Ge, G. Gendt, M. Rothacher, C. Shi, and J. Liu, "Resolution of GPS carrier-phase ambiguities in Precise Point Positioning (PPP) with daily observations," *J Geod* 82:389-399, 2008.
- [7] P. Héroux and J. Kouba, "GPS Precise Point Positioning Using IGS Orbit Products," *Phys. Chem. Earth (A)*, Vol. 26, No. 6-8, pp. 573-578, 2001.
- [8] C. Bruyninx and P. Defraigne, "Frequency transfer using GPS code and phases: short- and long-term stability," *Proc. 31st PTTI Meeting*, pp. 471-480, 1999.
- [9] G. Petit, "The TAIPPP pilot experiment," *Proc. EFTF-IFCS 2009 Joint Conference*, pp. 116-119, 2009.

